International Research Journal of Advanced Engineering and Science
ISSN (Online): 2455-9024

AgO–CuO Composite Catalyst Enabling Efficient and Selective Nitrate-to-Ammonia Conversion

Cheng Xiang Wang[1], JiaXin Liu[1], Rui Zhu[1], Peng Yi Zhao[1], Hua-Jun Shawn Fan[1,2]*
[1]College of Chemical Engineering, Sichuan University of Science and Engineering, Zigong City, Sichuan Province, P. R. China, 64300
[2]School of Natural Sciences and Mathematics, Claflin University, Orangeburg, SC 29115, USA

***Abstract*—** *By introducing silver oxide to construct an AgO-CuO composite catalytic system, the structural characteristics and NO_3RR performance were systematically studied. In the system of 0.5 M KOH+0.01 M KNO_3, the catalyst exhibits good catalytic performance at a potential of -0.5 V (vs. RHE), with an ammonia yield of 2302.17 $\mu g \cdot h^{-1} \cdot mg^{-1}$ and an FE of 72.26%. It exhibits better performance than 0.1 M KOH in 0.5 M KOH, and also shows good catalytic performance in the 0.5 M K_2SO_4+0.01 M KNO_3 system. Compared with single CuO or AgO catalysts, AgO CuO catalysts exhibit higher current density, superior ammonia yield, Faraday efficiency, and good long-term operational stability. Further research has found that the introduction of AgO not only improves the charge transfer ability of the catalyst, but also effectively regulates the adsorption behavior of nitrate and its reducing intermediates on the electrode surface, thereby suppressing hydrogen evolution side reactions and promoting the selective conversion of nitrate to ammonia.*

***Keywords*—** *Copper based catalyst; Nitrate reduction; Ammonia synthesis; Electrocatalysis; Precious metals.*

I. INTRODUCTION

Ammonia (NH_3) is an important chemical raw material for the production of fertilizers, chemicals, and pharmaceuticals, and is also considered a promising carbon free energy carrier[1-2]. At present, the industrial production of NH_3 largely relies on the Haber Bosch process, which reacts with nitrogen (N_2) and hydrogen (H_2) in the presence of iron-based catalysts at high temperatures (350-550 ℃) and high pressures (150-350 atm)[3]. The Haber Bosch process accounts for 1% - 2% of global energy production and approximately 1.6% of global carbon dioxide emissions[4-7]. On the other hand, due to the combustion of fossil fuels, excessive use of nitrogen fertilizers, and the emission of NO_3^- from industrial waste, NO_3^- has become one of the most widely distributed water pollutants in the world, posing a serious threat to ecological security and human health[8-10].

Therefore, it is essential to develop efficient and sustainable NH_3 production routes under environmental conditions. In recent years, the electrochemical nitrate reduction reaction (NO_3RR) powered by renewable energy has been considered a clean and sustainable method for generating NH_3 at room temperature[11]. Meanwhile, NO_3RR also provides a feasible approach to solving water pollution problems[12]. Unfortunately, due to the complex eight electron, nine proton process involved in the conversion of NO_3^- to NH_3, and the fact that the electroreduction of NO_3^- can generate various by-products through multiple reaction pathways, the kinetics and selectivity of NH_3 production from NO_3RR are poor[13-17]. Developing highly active and selective NO_3RR electrocatalysts is particularly important and urgent[18]. So far, copper is one of the most promising candidates for electrochemical NO_3RR conversion to NH_3. However, the NO_3RR performance of copper catalysts is still too low to meet the requirements of practical applications. Copper based catalysts typically have poor adsorption energy for NO_3RR and reaction intermediates on their surfaces, resulting in poor intrinsic activity and NH_3 selectivity[19-23].

This chapter takes copper based catalytic materials as the research object, constructs an AgO CuO composite catalytic system by introducing silver oxide, and systematically studies its structural characteristics and electrochemical nitrate reduction performance. AgO CuO catalyst was prepared using a reasonable synthesis method, and the crystal structure, microstructure, and surface chemical state of the material were systematically characterized by XRD, SEM, TEM, and XPS. The results indicate that AgO and CuO form close contact at the interface, successfully constructing a p-p type semiconductor heterojunction. There is a significant interface electronic interaction between multivalent Ag species and CuO. The activity, selectivity, and stability of AgO CuO catalyst in nitrate electroreduction reaction were systematically evaluated by electrochemical testing methods such as linear sweep voltammetry, cyclic voltammetry, and chronoamperometry.

The experimental results showed that in the system of 0.5 M KOH+0.01 M KNO_3, the catalyst exhibited good catalytic performance at a potential of -0.5 V, with an ammonia yield of 2302.17 $\mu g \cdot h^{-1} \cdot mg^{-1}$ and a Faraday efficiency of 72.26%. Compared to single CuO or AgO catalysts, AgO-CuO has higher current density, superior ammonia generation Faraday efficiency, and good long-term operational stability. Further research has found that the introduction of AgO not only improves the charge transfer ability of the catalyst, but also effectively regulates the adsorption behavior of nitrate and its reducing intermediates on the electrode surface, thereby suppressing hydrogen evolution side reactions and promoting the selective conversion of nitrate to ammonia. This study provides experimental basis and theoretical reference for the rational design of copper based nitrate electroreduction catalysts, and also provides new research ideas for the treatment of nitrate pollution in water bodies and the green preparation of ammonia.

1 Experimental section

1.1 Preparation of catalyst

Cheng Xiang Wang, JiaXin Liu1, Rui Zhu, Peng Yi Zhao, and Hua-Jun Shawn Fan, "AgO–CuO Composite Catalyst Enabling Efficient and Selective Nitrate-to-Ammonia Conversion," *International Research Journal of Advanced Engineering and Science*, Volume 11, Issue 2, pp. 152-162, 2026.

International Research Journal of Advanced Engineering and Science
ISSN (Online): 2455-9024

(1) Synthesis of CuO nanosheets

Dissolve 3.0 g of copper nitrate trihydrate ($Cu(NO_3)_2 \cdot 3H_2O$) in 25 mL of deionized water and stir magnetically for 30 minutes to form a uniform copper nitrate solution. Weigh 10 g of sodium hydroxide (NaOH) to a volume of 50 mL in a volumetric flask, slowly add the NaOH solution dropwise to the copper nitrate solution under vigorous stirring, and continue stirring for 30 minutes to obtain a blue flocculent precipitate. Transfer the mixed precursor solution to a reaction vessel and react at 200 ° C for 2 hours. After natural cooling to room temperature, collect the obtained product by centrifugation and wash it repeatedly with deionized water several times, then dry it overnight at 60 ° C. Heat the dried powder in a muffle furnace at a heating rate of 2 ℃ min^{-1} in an air atmosphere to 350 ℃, calcine for 2 hours, and finally obtain CuO nanosheets with good crystallinity.

(2) Synthesis of AgO CuO Heterojunction Catalyst

Weigh 0.2 g of CuO nanosheets prepared above, disperse them in 50 mL of deionized water, and sonicate for 30 min to obtain a uniform suspension. According to the target silver loading amount (5 wt%), 0.016 g of silver nitrate (AgNO3) was weighed and dissolved in 10 mL of deionized water. Then, the AgNO3 solution was slowly added dropwise to the CuO suspension and stirred in the dark for 1 hour to fully adsorb AgNO3 onto the CuO surface.

After adsorption is complete, under continuous stirring, add 0.1 M dilute NaOH solution dropwise to the above mixture to adjust the pH value of the system to 9-10. At this point, Ag^+ is deposited on the surface of CuO in the form of Ag_2O or AgOH. Continue to stir the suspension in the dark for 3 hours under this pH condition. After the reaction is complete, centrifuge the precipitate and wash it three times with deionized water and anhydrous ethanol to remove unreacted ions. Dry the collected product overnight in a 60 ° C vacuum drying oven.

Place the dried precursor powder in a ceramic boat and place it in a tube furnace for calcination treatment under an oxygen atmosphere. Firstly, the temperature was raised from room temperature to 350 ° C at a rate of 2 ° C min^{-1} and kept at this temperature for 2 hours. Oxygen was maintained in circulation to allow the sample to cool naturally to room temperature, resulting in the formation of AgO CuO heterostructure nanocatalysts.

1.2 Electrochemical nitrate reduction performance test

By adjusting the pH and nitrate concentration of the electrolyte, the impact of reaction circumstances on ammonia generation was investigated in the NO3RR performance test. By adjusting the pH of the solution to investigate the effects of neutral and alkaline environments on reaction kinetics and product selectivity, and setting different nitrate concentrations to study the effect of reactant concentration on ammonia generation rate. Perform constant potential electrolysis under fixed potential conditions and quantitatively analyze the generated ammonia and other by-products to systematically evaluate the effects of different pH and nitrate concentrations on the yield and Faraday efficiency of electrocatalytic ammonia production.

The electrochemical response signals were recorded by the CHI-760E electrochemical workstation. Using an H-type electrolytic cell equipped with Nafion 117 membrane, the initial volume of electrolyte is 50 mL.

Under neutral conditions, the measured potential is measured using a saturated calomel electrode (SCE) as the reference electrode; Under alkaline conditions, the measured potential is based on the Hg/HgO electrode as the reference electrode. The counter electrode is a platinum plate electrode, and the working electrode is a carbon paper loaded with a catalyst.

The linear sweep voltammetry (LSV) test has a scan rate of 50 mV s^{-1}, a constant potential test reaction time of 1 hour, and a stirring rate of 300 rpm. Double layer capacitors (Cdl) are obtained by performing cyclic voltammetry (CV) scans at different scan rates (20, 30, 40, 50, 60, 70, 80, 90 mV s^{-1}) within the non Faradaic potential range. The Cdl value is obtained by fitting the linear relationship between current density and scan rate at a specific potential.

II. Results and Discussion

2.1 Characterization of catalyst morphology and structure

Firstly, the crystal structure of the catalyst was characterized using XRD. As shown in Figure 1, clear diffraction peaks appear at positions 32.5 °, 35.5 °, 38.7 °, 48.7 °, 53.5 °, 58.3 °, 61.5 °, and 66.2 °, corresponding to the (110), (-111), (111), (-202), (020), (202), (-113), and (022) crystal planes of CuO (PDF # 45-0937), indicating that the prepared CuO has good crystallinity.

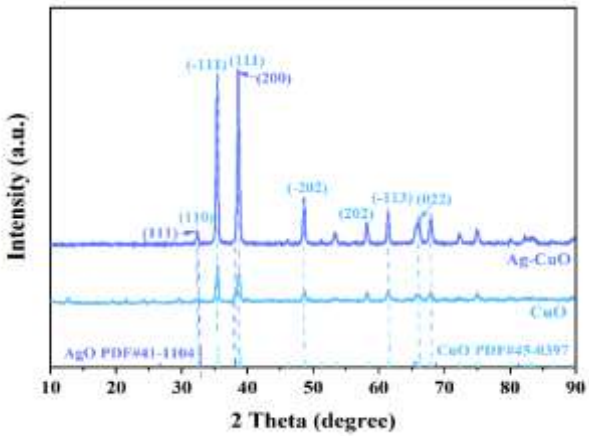

Figure 1. The XRD spectra of AgO-CuO and CuO

The diffraction peak of the composite material catalyst AgO-CuO is basically consistent with CuO and matches AgO (PDF#41-1104). The results indicate that AgO was successfully introduced into the CuO structure and formed a composite system. In addition, compared with pure CuO, the intensity of some diffraction peaks in the composite material changes, indicating that the introduction of AgO has a certain impact on the crystal structure of CuO and may form a tight heterogeneous interface between the two.

Further study the morphological characteristics of the catalyst and observe its microstructure using SEM. From Figure 2 (a), it can be seen that CuO is a structure formed by the stacking of irregular nanoparticles, with a relatively smooth surface. After introducing AgO, the surface of AgO CuO

Cheng Xiang Wang, JiaXin Liu1, Rui Zhu, Peng Yi Zhao, and Hua-Jun Shawn Fan, "AgO–CuO Composite Catalyst Enabling Efficient and Selective Nitrate-to-Ammonia Conversion," *International Research Journal of Advanced Engineering and Science*, Volume 11, Issue 2, pp. 152-162, 2026.

International Research Journal of Advanced Engineering and Science
ISSN (Online): 2455-9024

composite material becomes rougher (Figure 2 (b-d)) and forms a more uniform nanostructure, which is conducive to exposing more active sites and enhancing the electrochemical reaction activity of the catalyst.

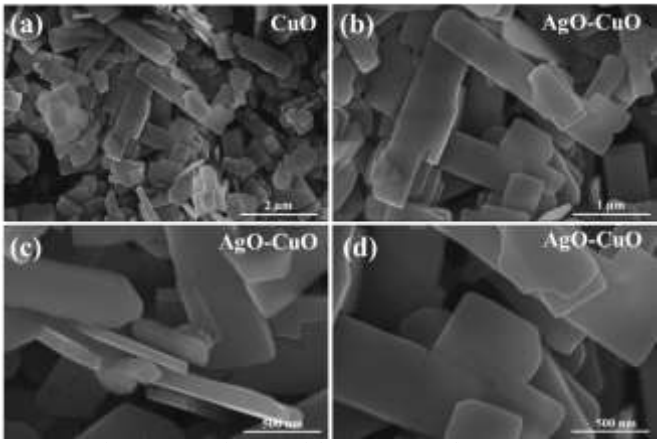

Figure 2. SEM images of the (a) CuO, (c-d) AgO-CuO

Analyze the microstructure of the catalyst through TEM. The TEM image shown in Figure 3 (a-b) shows that AgO nanoparticles are uniformly dispersed on the surface of CuO and form close contact with it, constructing a distinct heterojunction interface. Clear lattice fringes can be observed through HRTEM in Figure 3 (c), with a lattice spacing of approximately 0.252 nm, corresponding to the (111) crystal plane of CuO, while the lattice fringes of approximately 0.238 nm belong to the (002) crystal plane of AgO. These results further indicate the successful construction of a heterostructure interface between AgO and CuO, which facilitates the transfer of electrons between different components, thereby improving catalytic performance.

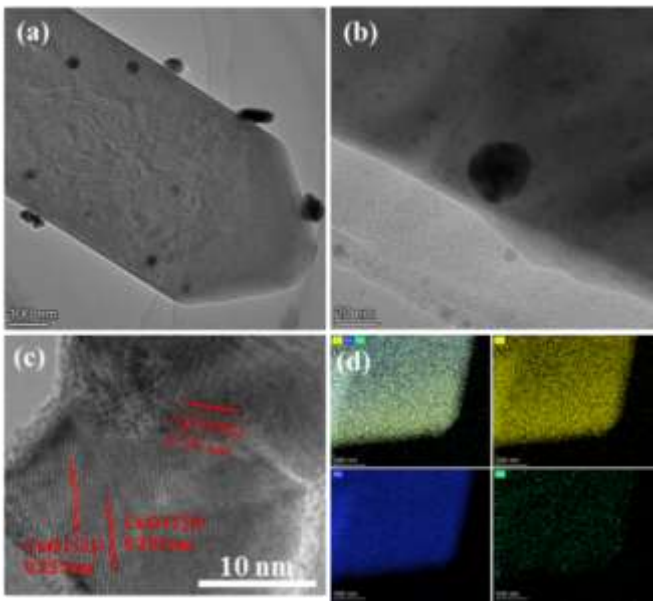

Figure 3. (a-b) TEM images of AgO-CuO, (c) HRTEM image of AgO-CuO, and (d) Corresponding EDS element mapping

Perform element mapping analysis through EDS to explore the distribution of elements. As shown in Figure 3 (d), Ag, Cu, and O elements are uniformly distributed throughout the catalyst without obvious element enrichment or separation, indicating that AgO is successfully loaded on the CuO surface and forms a stable composite structure. This uniform distribution of elements is beneficial for constructing more effective heterogeneous interfaces, thereby increasing the number of active sites in the catalyst.

In addition, the chemical valence states of various elements in the catalyst were analyzed by XPS. As shown in Figure 4, the XPS full spectrum shows that the sample mainly contains Ag, Cu, and O elements. In Figure 5 (a), the high-resolution spectrum of Ag 3d shows two characteristic peaks at 368.46 eV and 374.47 eV, corresponding to Ag $3d_{5/2}$ and Ag $3d_{3/2}$, respectively, indicating that Ag mainly exists in the form of AgO. Compared with a single component, some peak positions in the composite material show slight shifts, indicating a significant electronic interaction between AgO and CuO. This interface electronic coupling helps to regulate the electronic structure of the catalyst, thereby promoting electron transfer in the NO_3RR process and improving ammonia generation efficiency. According to Figure 5 (b), clear peaks appear at approximately 934.42 eV and 954.23 eV in the high-resolution Cu 2p spectrum, corresponding to the characteristic peaks of Cu $2p_{3/2}$ and Cu $2p_{1/2}$ of Cu^{2+}, accompanied by distinct satellite peaks, indicating the presence of CuO[23]. It is consistent with the results in Cu LMM (Figure 5 (c)).

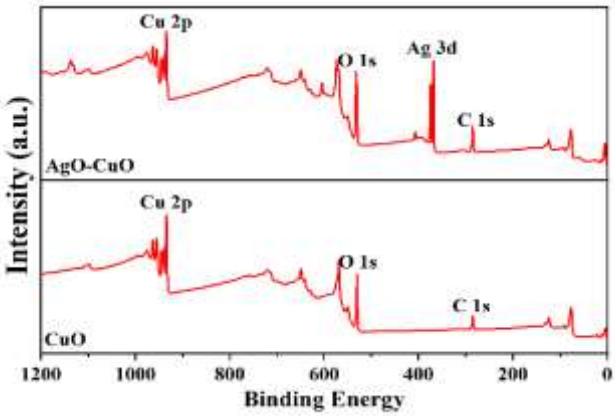

Figure 4. XPS total spectra of AgO-CuO and CuO

In the high-resolution O 1s spectrum (Figure 3-5 (d)), three different types of oxygen can be observed. Among them, the peak at 529.91 eV belongs to lattice oxygen (OL) in metal oxides, mainly derived from the CuO and AgO lattice structures; The peak at 531.79 eV is usually associated with surface adsorbed oxygen or defect oxygen, which are often related to oxygen vacancies (OV) on the material surface; At a peak of 532.69 eV, it is generally the adsorption of hydroxyl OH or water molecules. The comparatively high surface adsorption of oxygen and defect oxygen suggests that there are some oxygen vacancies on the material's surface, which aids in encouraging the adsorption and activation of reactants and improving the electrocatalytic effect.

In addition, compared to pure CuO, there is a slight shift in the peak positions of O 1s and Cu LMM in AgO-CuO composite materials, indicating a certain electronic coupling

Cheng Xiang Wang, JiaXin Liu1, Rui Zhu, Peng Yi Zhao, and Hua-Jun Shawn Fan, "AgO–CuO Composite Catalyst Enabling Efficient and Selective Nitrate-to-Ammonia Conversion," *International Research Journal of Advanced Engineering and Science*, Volume 11, Issue 2, pp. 152-162, 2026.

International Research Journal of Advanced Engineering and Science
ISSN (Online): 2455-9024

effect between AgO and CuO. This interface electronic coupling effect can change the electronic structure of the catalyst surface and improve the NO_3RR reaction process of the catalyst. From the above characterization, it can be seen that AgO and CuO construct a stable heterostructure interface, which can provide sufficient active sites and promote charge transfer at the interface, providing a structural basis for electrocatalytic nitrate reduction to ammonia reaction.

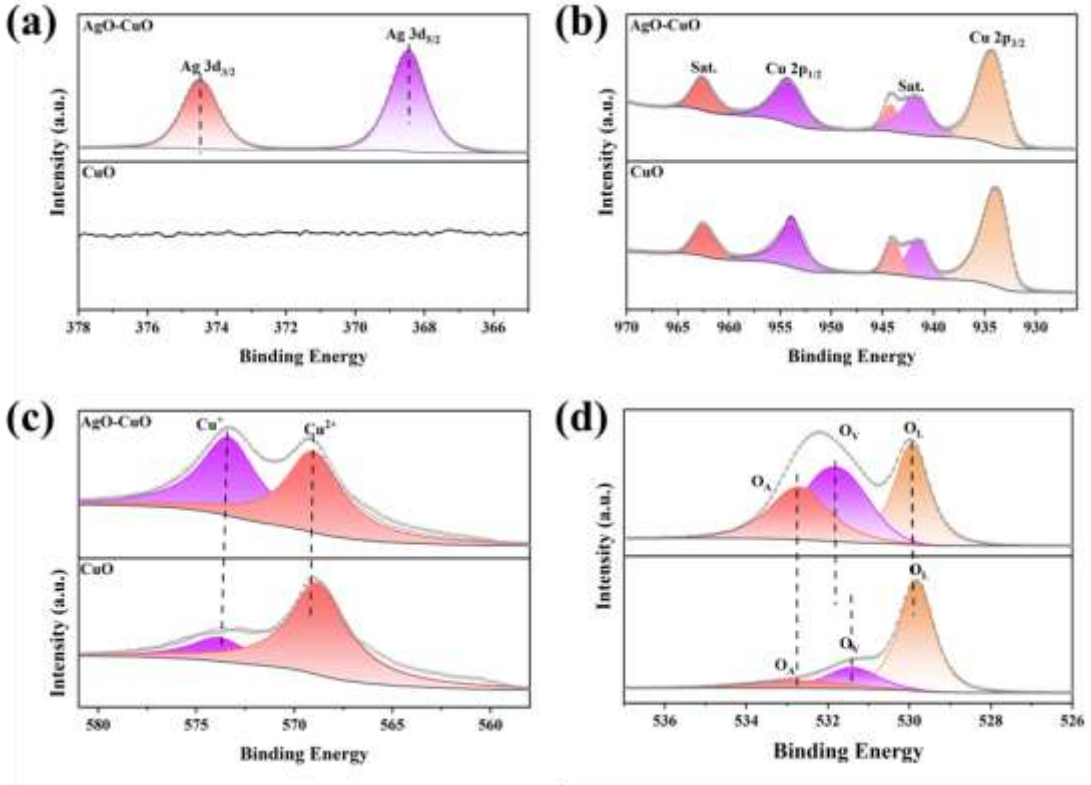

Figure 5. XPS spectra of AgO-CuO and CuO: (a) Ag 3d, (b) Cu 2p, (c) Cu LMM, (d) O 1s

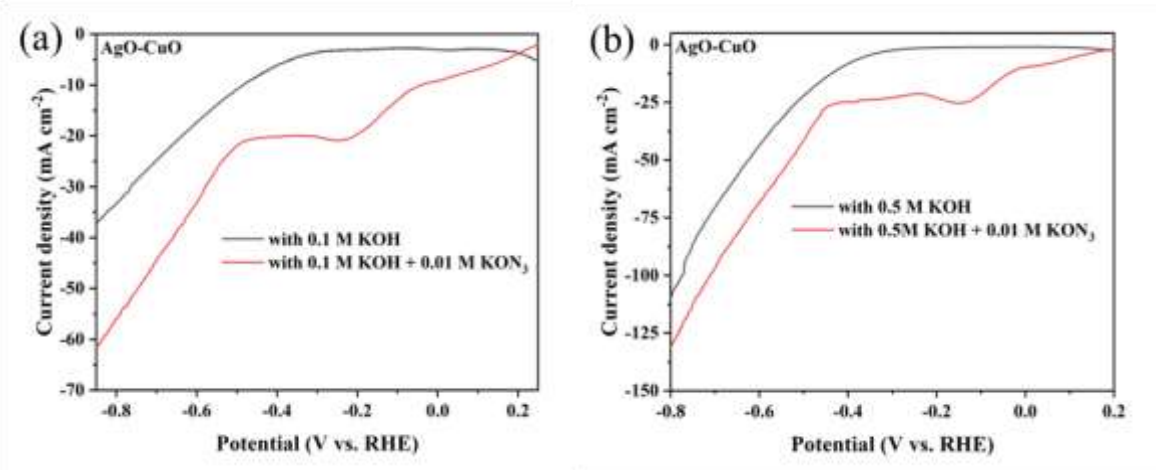

Figure 6. LSV curves of AgO-CuO in (a) 0.1 M KOH and (b) 0.5 M KOH electrolytes with or without NO3-

2.2 Study on the electrocatalytic nitrate reduction performance

In an electrolyte containing only 0.1 M KOH, the current density of the AgO CuO electrode gradually increases with the negative shift of the potential (Figure 6 (a)). When the potential is below -0.2V, the current density is -5 mA cm ². When the potential is -0.8V, the current density increases to -60 mA cm ². When the KOH concentration reaches 0.5M, the current density increases at the same potential (Figure 6 (b)). At this point, the current density at -0.8V is -125 mA cm ², significantly higher than -65 mA cm ² in 0.1 M KOH. This is due to the electrolyte's increased conductivity, which lessens Ohmic polarization and improves electrode reaction kinetics. This indicates that increasing electrolyte concentration is beneficial for improving the charge transfer efficiency on the electrode surface.

In the potential range of -0.5 V to -0.8 V, the increase in current density in the electrolyte containing NO_3^- is significantly greater than that in the blank electrolyte, indicating that nitrate reduction reaction dominates. However, the sharp

Cheng Xiang Wang, JiaXin Liu1, Rui Zhu, Peng Yi Zhao, and Hua-Jun Shawn Fan, "AgO–CuO Composite Catalyst Enabling Efficient and Selective Nitrate-to-Ammonia Conversion," *International Research Journal of Advanced Engineering and Science*, Volume 11, Issue 2, pp. 152-162, 2026.

increase in current density at -0.8 V may be related to the promotion of hydrogen evolution reaction, and there is a competitive relationship between the two. AgO-CuO catalyst has good charge transfer ability in high concentration KOH electrolyte and strong electrocatalytic activity for nitrate reduction. It is preliminarily believed that the optimal activity potential range is -0.5 V to -0.8 V. The selectivity and reaction mechanism will be determined through quantitative analysis of the products.

To verify the above judgment and further evaluate the catalytic performance of AgO-CuO for nitrate reduction, i-t tests were conducted at different potentials for 1 hour. As shown in Figure 7, the FE at both concentrations exhibited a volcanic distribution, and the NH_4^+ yield gradually increased with the increase of negative potential. The AgO-CuO catalyst achieved the highest FE of 72.56% in a 0.5 M KOH electrolyte at a potential of -0.5 V (Figure 7 (a)), while in a 0.1 M KOH electrolyte, the optimal FE potential was negatively shifted to -0.6 V, and the highest FE efficiency was 51.27% (Figure 7 (b)). This potential difference indicates that electrolyte concentration has a significant impact on the competitive equilibrium between nitrate reduction reaction (NO_3RR) and hydrogen evolution reaction (HER). In terms of NH_4^+ yield, the 0.5 M KOH solution is significantly higher than the 0.1 M KOH solution, which is consistent with the selectivity of the products described below, indicating that higher concentrations of KOH accelerate intermediate conversion and reduce intermediate volume accumulation.

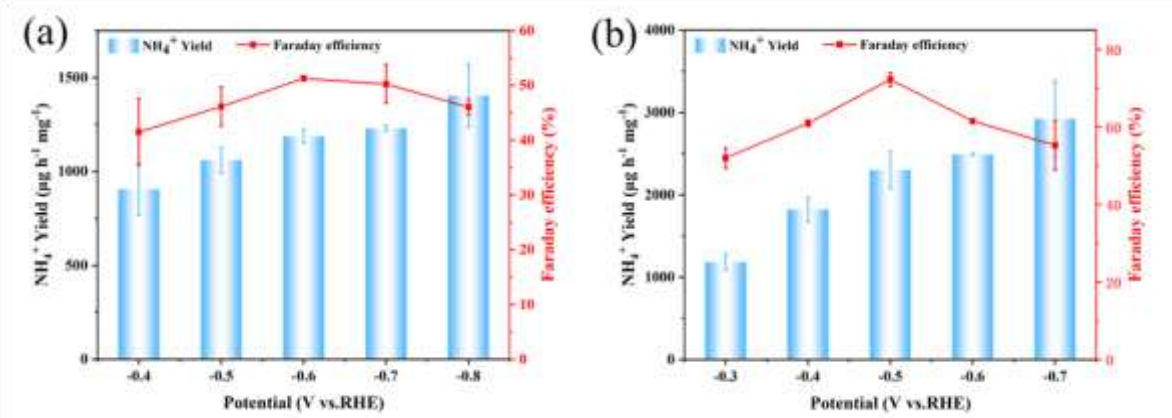

Figure 7. Ammonia yield and FE of AgO-CuO at different potentials in (a) 0.1 M KOH + 0.01 M KNO_3 and (b) 0.5 M KOH + 0.01 M KNO_3 electrolytes

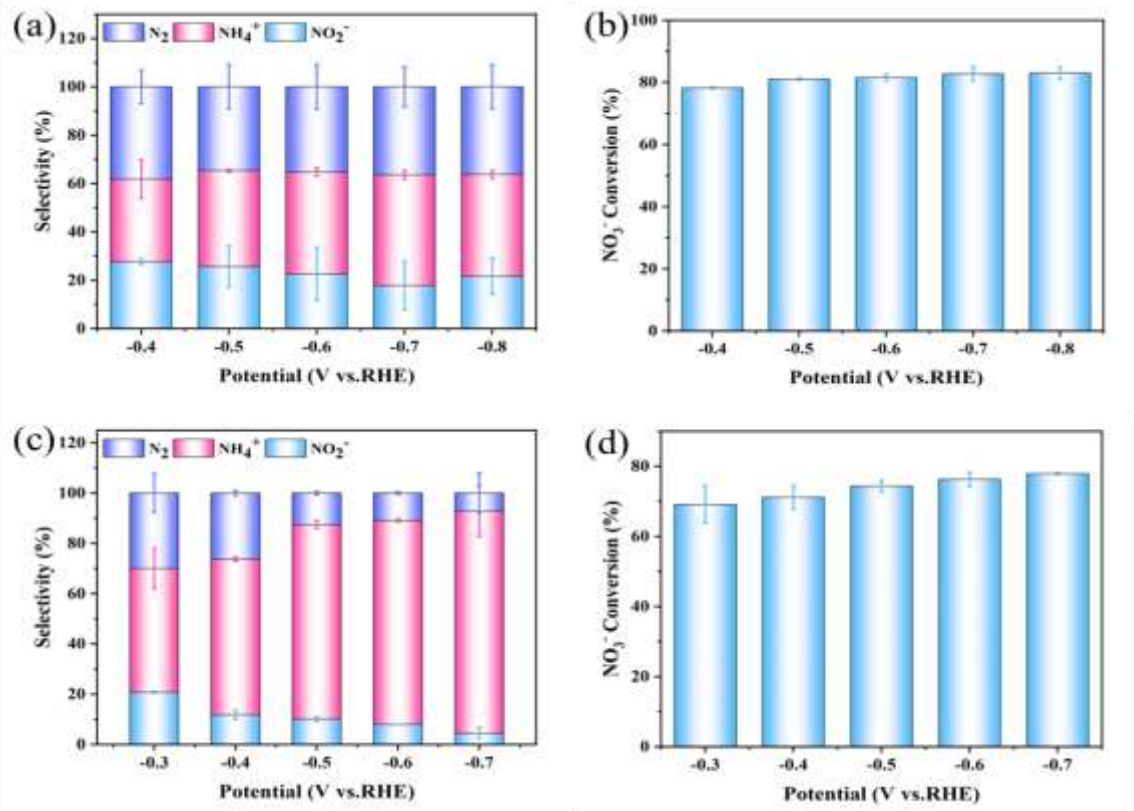

Figure 8. Selectivity of products and nitrate conversion of AgO-CuO in (a) 0.1 M KOH + 0.01 M KNO_3, (b) 0.5 M KOH + 0.01 M KNO_3 electrolytes at different potentials

Cheng Xiang Wang, JiaXin Liu1, Rui Zhu, Peng Yi Zhao, and Hua-Jun Shawn Fan, "AgO–CuO Composite Catalyst Enabling Efficient and Selective Nitrate-to-Ammonia Conversion," *International Research Journal of Advanced Engineering and Science*, Volume 11, Issue 2, pp. 152-162, 2026.

International Research Journal of Advanced Engineering and Science
ISSN (Online): 2455-9024

In a 0.1 M KOH solution, there was no significant change in the selectivity of the three products at different potentials, maintaining low NH_4^+ selectivity and high N_2 and NO_2^- selectivity (Figure 8 (a)). The conversion rate of NO_3^- was around 80% (Figure 8 (b)). However, in a 0.5 M KOH solution, as shown in Figure 8 (c), as the potential gradually increases, the selectivity of NH_4^+ also increases, while the selectivity of N_2 and NO_2^- gradually decreases. At the maximum FE potential (-0.5 V), the selectivity of NH_4^+, N_2, and NO_2^- is 77.40%, 12.46%, and 10.14%, respectively; At -0.7 V, the selectivity of NH_4^+ reached 77.40%, and the conversion rate of NO_3^- was also around 80% (Figure 8 (d)). This indicates that higher concentrations of KOH not only improve mass transfer and reaction kinetics, but also promote the deep reduction pathway of nitrate to the target product ammonia by optimizing the electrode surface microenvironment, while inhibiting the accumulation of harmful intermediates.

Analysis found that in a low concentration electrolyte of 0.1 M KOH, the ion strength is low, and the electromigration and mass transfer of NO_3^- to the electrode surface are somewhat limited. Therefore, a higher overpotential (-0.6 V) is required to overcome mass transfer resistance and effectively activate nitrate ions. At the same time, the proton supply is limited at low concentrations, which inhibits the hydrogen evolution reaction (HER), allowing NO_3RR to maintain high selectivity at relatively negative potentials. When the concentration of KOH is increased to 0.5 M, the conductivity of the electrolyte significantly increases, and the ion mass transfer efficiency is greatly improved. NO_3^- can obtain sufficient supply at a positive potential (-0.5 V) without the need for additional overpotential to overcome mass transfer barriers. In addition, although high concentrations of OH^- are theoretically beneficial for HER, HER has not yet occurred violently at a moderate potential of -0.5 V, while NO_3RR has sufficient driving force. At the same time, the enhanced ion strength optimizes the adsorption energy of reaction intermediates by affecting the double-layer structure on the electrode surface, enabling efficient NO_3RR at lower overpotentials. The results indicate that electrolyte concentration significantly affects the optimal reaction potential of the catalyst by regulating ion mass transfer efficiency, electrode surface microenvironment, and HER competition intensity. Mass transfer limitation dominates at low concentrations, requiring a more negative potential to drive the reaction; Mass transfer is improved at high concentrations, and the reaction can proceed efficiently at a corrected potential. KOH concentration achieves higher ammonia synthesis efficiency by improving mass transfer, kinetics, and selectivity.

As shown in Figure 9 (a), in a 0.1 M KOH solution, with the increase of NO_3^- concentration, the LSV curve of the catalyst suddenly increases after 0.3 V, but there is no trend of continuous increase in current density. It shows a flat curve at -0.2 V, and the overall curve change is not significant, indicating current response saturation. Indicating that nitrate reduction reactions may be limited by mass transfer processes or electrode interface reaction kinetics. In contrast, in a 0.5 M KOH solution, the current density increases more sharply after 0.4 V and tends to flatten at -0.4 V (Figure 9 (b)). The reason for this is that as the concentration of nitrate increases, the number of NO3- species that can participate in electrochemical reactions in the reaction system gradually increases, but the number of effective active sites on the catalyst surface is limited. As the adsorption sites on the catalyst surface gradually become occupied, further increasing the nitrate concentration does not significantly improve the reaction rate. Therefore, the LSV curve no longer shows a significant increase and exhibits an approximately flat current response.

Due to the direct proportionality between C_{dl} and the electrochemical active area of the electrode, measuring C_{dl} allows for a relative comparison of the number of active sites on different catalysts. Measure the CV curves of catalysts at scan rates of 20, 40, 60, 80, 100, and 120 mV s^{-1} respectively, and further measure the C_{dl} of AgO CuO in different electrolytes. The CV curves of AgO CuO in 0.5 M KOH+0.01 M KNO_3 electrolyte are shown in Figure 10 (a), and the CV curves in 0.1 M KOH+0.01 M KNO_3 electrolyte are shown in Figure 3-10 (c). From Figure 10 (b) and Figure 3-10 (d), it can be seen that the C_{dl} of AgO-CuO in 0.5 M KOH is greater than that in 0.1 M KOH, with values of 0.87 mF cm^{-2} and 0.71 mF cm^{-2}, respectively. And higher C_{dl} usually means more active sites are exposed, which is conducive to the adsorption and reduction of NO_3^-, and may result in higher ammonia yield.

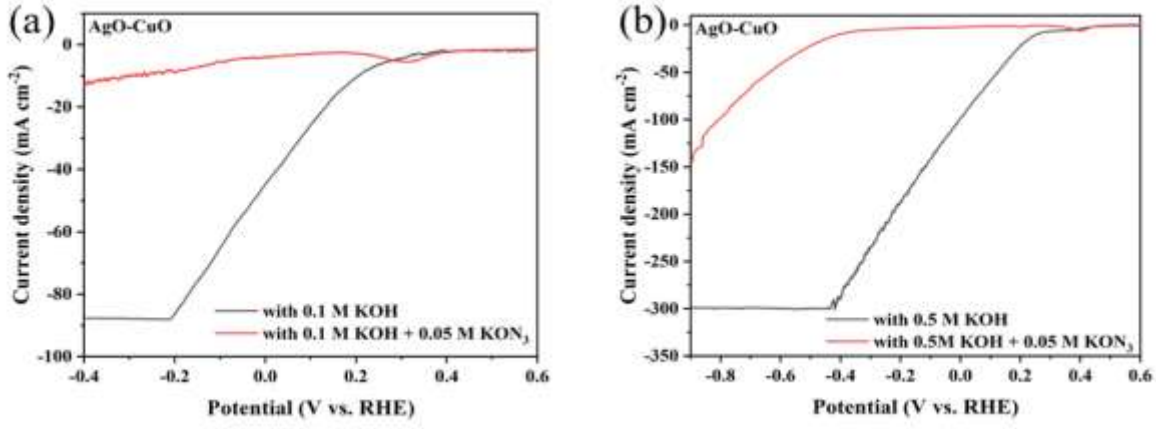

Figure 9. In 0.1 M KOH + 0.01 M KNO_3 electrolyte, LSV curves of AgO-CuO in the presence and absence of NO_3^-

Cheng Xiang Wang, JiaXin Liu1, Rui Zhu, Peng Yi Zhao, and Hua-Jun Shawn Fan, "AgO–CuO Composite Catalyst Enabling Efficient and Selective Nitrate-to-Ammonia Conversion," *International Research Journal of Advanced Engineering and Science*, Volume 11, Issue 2, pp. 152-162, 2026.

International Research Journal of Advanced Engineering and Science
ISSN (Online): 2455-9024

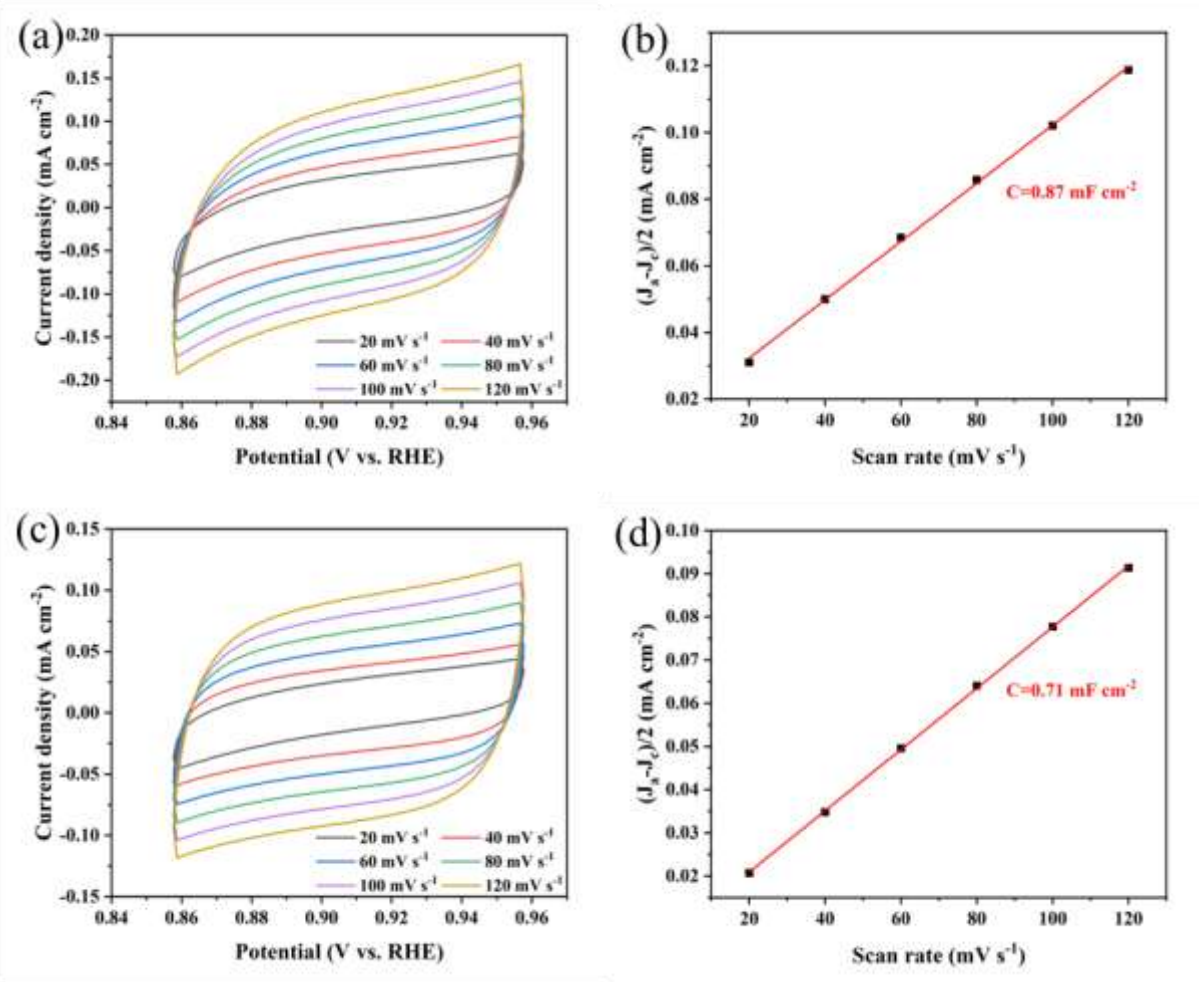

Figure 10. CV curves of AgO-CuO at different scan rates in the non-Faradaic region in (a-b) 0.5 M KOH + 0.01 M KNO3 and (c-d) 0.1 M KOH + 0.01 M KNO3 electrolytes, and their corresponding Cdl fitting curves

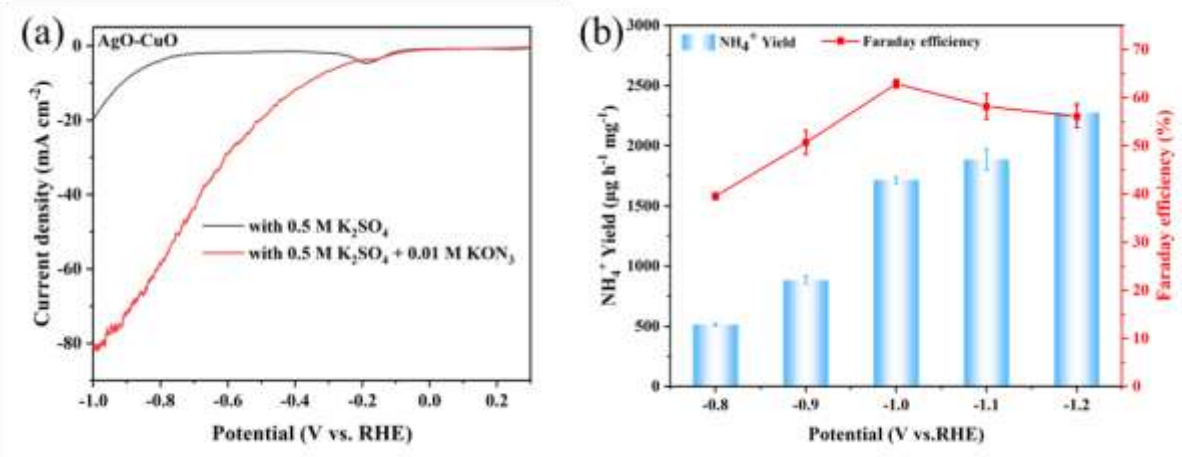

Figure 11. In 0.1 M KOH + 0.01 M KNO_3 electrolyte, (a) LSV curves of AgO-CuO in the presence and absence of NO_3^-, (b) ammonia yield and FE of AgO-CuO at different potentials

The LSV curves were measured in a 0.5M electrolyte with and without 0.01 M KNO_3, as shown in Figure 11 (a): in the positive potential range (> -0.2 V), the two curves basically overlap, indicating that the reduction of NO_3^- has not been effectively initiated within this potential range, and the current mainly comes from HER. When the potential shifts to below -0.4 V, the current density of the system containing NO_3^- begins to be significantly higher than that of the blank system, and the difference gradually increases with the negative potential shift. When the potential shifts to -0.8 V, the current density of the system containing NO_3^- reaches -58.97 mA cm^{-2}, significantly higher than the blank system's -3.99 mA cm^{-2}. This difference

Cheng Xiang Wang, JiaXin Liu1, Rui Zhu, Peng Yi Zhao, and Hua-Jun Shawn Fan, "AgO–CuO Composite Catalyst Enabling Efficient and Selective Nitrate-to-Ammonia Conversion," *International Research Journal of Advanced Engineering and Science*, Volume 11, Issue 2, pp. 152-162, 2026.

International Research Journal of Advanced Engineering and Science
ISSN (Online): 2455-9024

is attributed to the contribution of the NO_3^- reduction reaction (NO_3RR), indicating that at lower potentials, NO_3RR and HER occur simultaneously, and the former's contribution significantly increases. Initial potential analysis: The initial potential of NO_3RR is about -0.2 V, below which NO_3^- begins to be reduced.

As shown in Figure 11 (b), with the negative shift of potential, the ammonia yield continues to increase, and FE shows a volcanic trend of first increasing and then decreasing. At -0.8 V, the FE is low (39.51%), attributed to insufficient driving force; -At 1.0 V, the peak value (62.86%) was reached, indicating that the competition between NO_3RR and HER reached optimal equilibrium at this potential; When the potential further shifts to -1.2 V, FE decreases to 56.1%, which is due to the intensified competition of HER under high overpotential, and a large number of electrons are used for hydrogen evolution rather than target product synthesis.

As the potential shifts negatively, the selectivity of NH_4^+ gradually increases, while the selectivity of NO_2^- and N_2 gradually decreases (Figure 12 (a)). The conversion rate of NO_3^- increased from 74.25% at -0.8 V to 86.86% at -1.2 V (Figure 12 (b)), indicating that the catalyst has good reducing ability for nitrate, and most of the NO_3^- was effectively converted. Based on the ammonia yield and selectivity data, most of the converted nitrate is converted to the target product NH_4^+, with a small amount converted to NO_2^- intermediates and N_2 by-products.

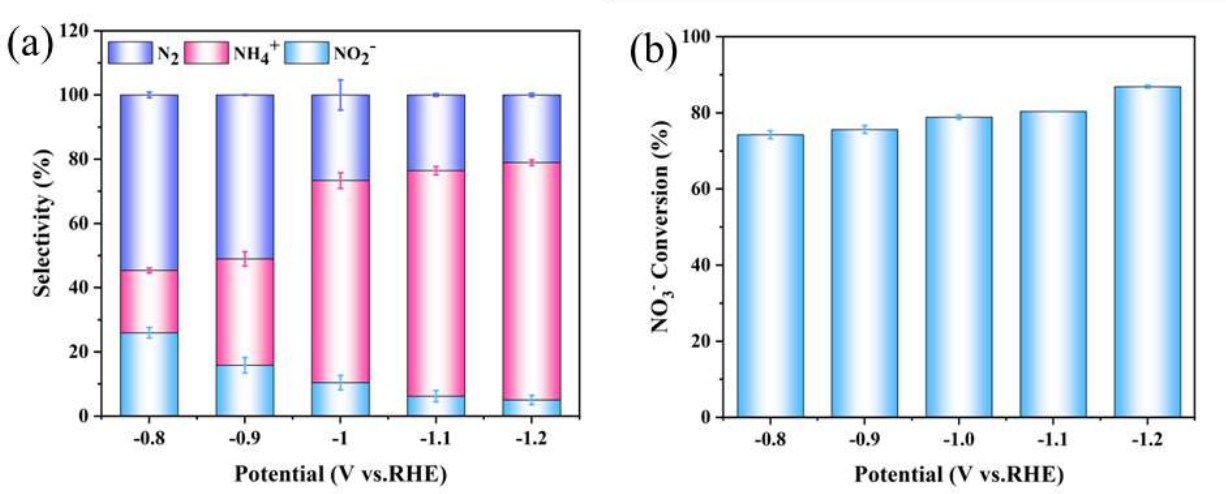

Figure 12. In 0.5 M K_2SO_4+0.01 M KNO_3 electrolyte, (a) Product selectivity, and (b) Nitrate conversion of AgO-CuO at different potentials

Measure the CV curves of AgO-CuO and CuO catalysts at scan rates of 20, 40, 60, 80, 100, and 120 mV s^{-1}, and further measure the C_{dl} of AgO CuO in different electrolytes. The CV curves of AgO CuO in 0.5 M K_2SO_4+0.01 M KNO_3 electrolyte are shown in Figure 13 (a), and the CV curves of CuO in 0.5 M K_2SO_4+0.01 M KNO_3 electrolyte are shown in Figure 13 (c). According to Figures 13 (b) and 13 (d), the C_{dl} of AgO CuO catalyst is 2.1 mF cm^{-2}, while that of pure CuO is 0.75 mF cm^{-2}. This result indicates that AgO-CuO heterostructures have a larger electrochemical active area, meaning that more active sites are exposed per unit geometric area. The introduction of AgO may alter the morphology or dispersion state of CuO. During the synthesis process, AgO nanoparticles were loaded onto the surface of CuO nanosheets, forming nanoscale heterogeneous interfaces. This structure effectively prevents the aggregation of CuO nanosheets, exposing active sites that may have been obscured, thereby increasing the electrochemical active area.

There is lattice mismatch and electronic structure reconstruction at the interface of AgO-CuO heterojunction, and the interface region itself may become a new active site. These interface sites have unique adsorption capabilities for NO_3^- and participate in the double-layer charge discharge process, contributing additional capacitance response. The loading of AgO nanoparticles on CuO surface increases the micro roughness of the electrode surface. The rough surface structure means a larger solid-liquid contact area, which exhibits higher double-layer charging current during CV scanning, reflecting higher C_{dl} values. The introduction of AgO may enhance the overall electronic conductivity of the composite material. Better conductivity enables more active sites inside the electrode to effectively participate in electrochemical reactions, resulting in higher capacitance response in C_{dl} testing.

As shown in Figure 14 (a), at -0.5 V (relative to RHE), the FE of AgO CuO is 72.26%, and the NH_3 production rate is 2302.17 μ g h^{-1} mg^{-1}. The FE of AgO and CuO are 56.09% and 62.47%, respectively, and the NH_3 production rates are 1752.17 μg h^{-1} mg^{-2} and 1602.17 μg h^{-1} mg^{-2}, respectively. The results showed that the catalytic performance of AgO-CuO was significantly better than that of single AgO and CuO. In order to eliminate potential interference from the electrocatalyst itself or external environment, control experiments were conducted in open circuit voltage and KOH electrolyte without KNO_3. The experimental results indicate that the amount of NH_3 generated can be neglected under open circuit voltage and NO_3^- free conditions (Figure 14 (b)).

Cheng Xiang Wang, JiaXin Liu1, Rui Zhu, Peng Yi Zhao, and Hua-Jun Shawn Fan, "AgO–CuO Composite Catalyst Enabling Efficient and Selective Nitrate-to-Ammonia Conversion," *International Research Journal of Advanced Engineering and Science*, Volume 11, Issue 2, pp. 152-162, 2026.

International Research Journal of Advanced Engineering and Science
ISSN (Online): 2455-9024

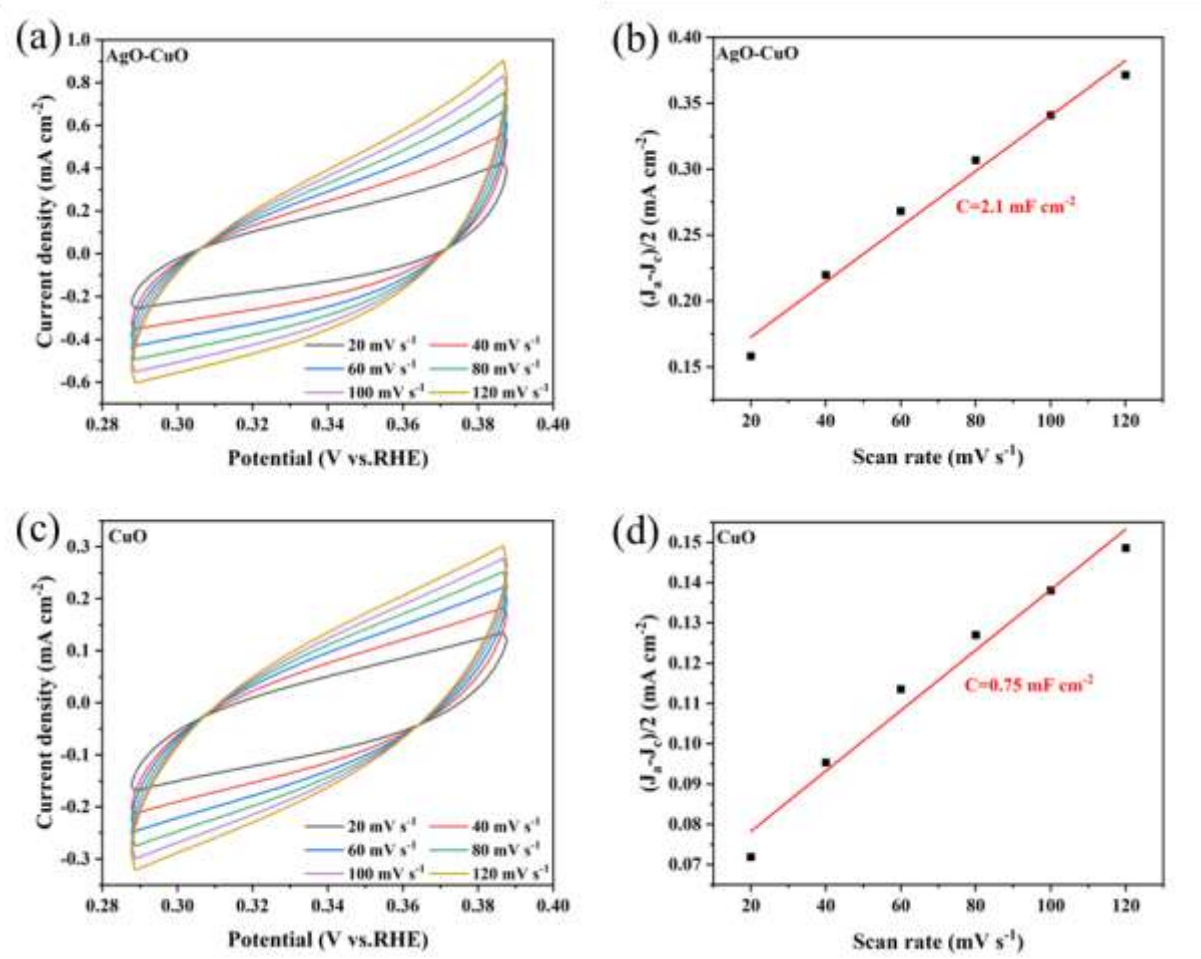

Figure 13. In 0.5 M K_2SO_4 + 0.01 M KNO_3 electrolyte, CV curves of (a-b) AgO-CuO and (c-d) CuO at different scan rates in the non-Faradaic region and their corresponding C_{dl} fitting curves

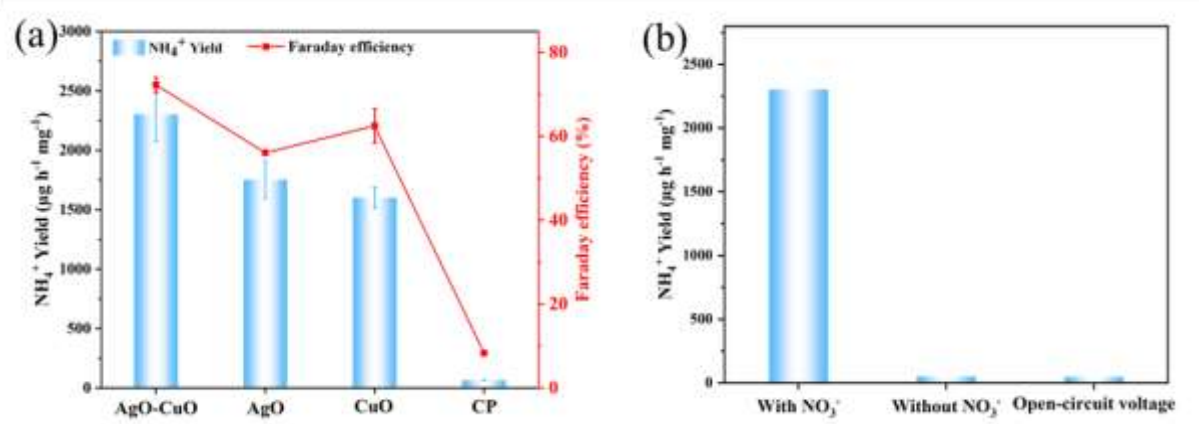

Figure 14. In 0.5 M K_2SO_4 + 0.01 M KNO_3 electrolyte, at a potential of -0.5 V vs RHE, (a) the ammonia yield and FE of AgO-CuO, AgO, CuO, and CP, (b) the ammonia yield of AgO-CuO with and without NO_3^- and at a given open-circuit voltage in the presence of NO_3^-

The stability of the catalyst was tested through continuous cyclic electrolysis experiments, with each cycle lasting for 1 hour at a potential of -0.5 V vs. RHE. As shown in Figure 15 (a), in the continuous cycle test, both FE and NH_3 yields showed slight fluctuations, but remained stable in 6 cycles; The conversion rate of NO_3^- also remained overall stable (Figure 15 (b)), indicating the excellent stability of AgO-CuO in NO_3RR.

Cheng Xiang Wang, JiaXin Liu1, Rui Zhu, Peng Yi Zhao, and Hua-Jun Shawn Fan, "AgO–CuO Composite Catalyst Enabling Efficient and Selective Nitrate-to-Ammonia Conversion," *International Research Journal of Advanced Engineering and Science*, Volume 11, Issue 2, pp. 152-162, 2026.

International Research Journal of Advanced Engineering and Science
ISSN (Online): 2455-9024

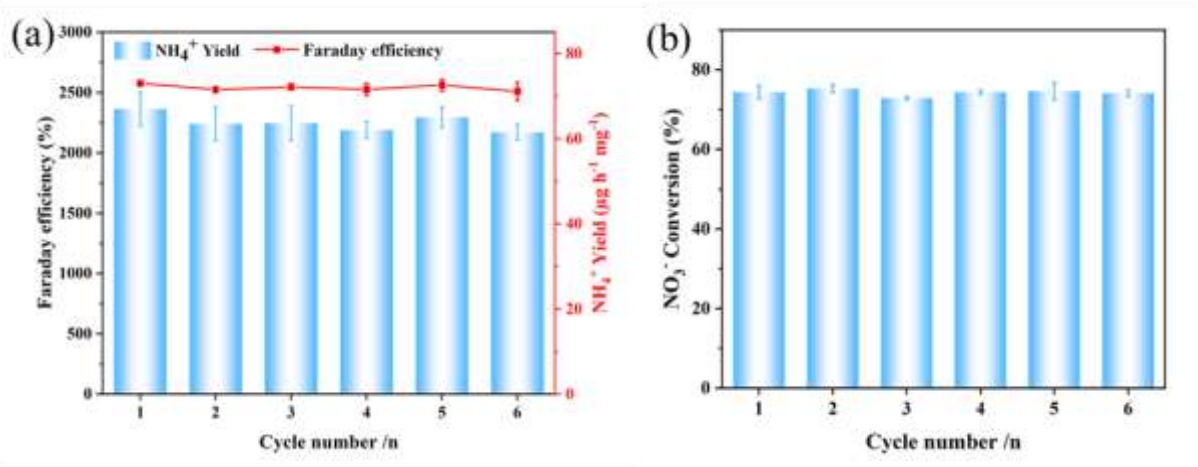

Figure 15. In 0.5 M K_2SO_4 + 0.01 M KNO_3 electrolyte, AgO-CuO after 6 cycles of electrolysis at -0.5 V vs RHE: (a) ammonia yield and FE, (b) NO_3^- conversion

III. Conclusion

This chapter systematically explores the electrocatalytic performance of AgO-CuO heterojunction catalyst for nitrate reduction to ammonia. By combining deposition precipitation method with oxygen atmosphere calcination, AgO nanoparticles are uniformly loaded on the surface of CuO nanosheets, and AgO-CuO heterostructures are successfully constructed. The catalyst exhibits better ammonia synthesis performance in 0.5 M KOH than in 0.1 M KOH. The optimal Faraday efficiency potential shifts positively from -0.6 V to -0.5 V, resulting in a significant improvement in energy efficiency; The ammonia yield and Faraday efficiency have both significantly improved. At the optimal reaction potential, the ammonia yield reached 2302.17 μg h^{-1} mg^{-1}, and the Faraday efficiency was 72.26%. The selectivity of NH_4^+, NO_2^-, and N_2 products were 77.40%, 10.14%, and 12.46%, respectively. The conversion rate of NO_3^- was 74.34%, attributed to the higher concentration of electrolyte improving mass transfer efficiency, optimizing reaction kinetics, accelerating intermediate conversion, and regulating the electrode surface microenvironment. As the concentration of NO_3^- further increases, the LSV curve tends to flatten, indicating that the reaction has entered the mass transfer control zone or the active site saturation zone. This suggests that further improving performance needs to start with enhancing mass transfer (such as using a flow electrolysis cell) or improving the intrinsic activity of the catalyst, rather than simply increasing the concentration of reactants. In the 0.5 M K_2SO_4 + 0.01 M KNO_3 system, the optimal reaction potential is -1.0 V, the ammonia yield reaches 1715.63 μg h^{-1} mg^{-1}, and the Faraday efficiency is 62.86%. The selectivity of NH_4^+, NO_2^-, and N_2 products were 62.94%, 10.43%, and 26.63%, respectively, and the conversion rate of NO_3^- was 78.86%. The results indicate that the catalyst also exhibits good catalytic activity under neutral conditions.

The AgO-CuO heterojunction exhibits superior comprehensive performance compared to pure CuO, and its excellent NO_3RR properties are attributed to the synergistic effect of high active site density and optimized intrinsic activity. The optimal electrolyte system was 0.5 M KOH, which achieved the highest ammonia selectivity and conversion rate under these conditions. This study provides experimental basis and theoretical reference for the design of efficient nitrate reduction catalysts for ammonia production and optimization of electrolyte systems.

Acknowledgments

This work was completed with the support of the advanced research platform of the College of Chemical Engineering, Sichuan University of Science & Engineering. Partial financial support was provided by the Yibin Libao New Materials Cooperation (#HX2021279 and #2024ZD003) and graduate scholarships.

References

[1] Elser J. A World Awash with Nitrogen [J]. Science (New York, NY), 2011, 334: 1504-5.
[2] Van Langevelde P H, Kstsounaros I, Koper M T M. Electrocatalytic Nitrate Reduction for Sustainable Ammonia Production [J]. Joule, 2021, 5(2): 290-4.
[3] Smith C, Hill A K, Torrente-Murciano L. Current and future role of Haber–Bosch ammonia in a carbon-free energy landscape [J]. Energy & Environmental Science, 2020, 13(2): 331-44.
[4] Mahmoos S, Alduhaish O, Ammar M, et al. Pt-modified Fe_3O_4 Supported on Ni Foam Nanocomposite for Electrocatalytic Nitrate Reduction to Ammonia [J]. Electrocatalysis, 2024, 15(1): 159-70.
[5] Ren T, Yu Z, Yu H, et al. Interfacial polarization in metal-organic framework reconstructed Cu/Pd/CuO_x multi-phase heterostructures for electrocatalytic nitrate reduction to ammonia [J]. Applied Catalysis B: Environmental, 2022, 318: 121805.
[6] Zhao X, Jiang Y, Wang M, et al. Optimizing Intermediate Adsorption via Heteroatom Ensemble Effect over RuFe Bimetallic Alloy for Enhanced Nitrate Electroreduction to Ammonia [J]. Advanced Energy Materials, 2023, 13(31): 2301409.
[7] Zhang Y, Xu M, Zhou J, et al. Concave Fe_2O_3 nanocubes with high-index facets for ammonia production from electrocatalytic nitrate reduction [J]. Chemical Communications, 2025, 61(7): 1395-8.
[8] Cao Y, Yuan S, Hai Y, et al. Amorphous Ni3B Promotes Electroreduction of Nitrate to Ammonia [J]. ACS Applied Materials & Interfaces, 2024, 16(47): 64807-15.
[9] Xu T, Wang Z, Zhu H, et al. Interface-engineered Co_3O_4 nano-islands on a Cu substrate for high-efficiency electrocatalytic nitrate-to-ammonia conversion [J]. Chemical Communications, 2025, 61(56): 10387-90.
[10] Feng X, Liu J, Kong Y, et al. Cu/Cu_xO/Graphdiyne Tandem Catalyst for Efficient Electrocatalytic Nitrate Reduction to Ammonia [J]. Advanced Materials, 2024, 36(44): 2405660.
[11] Da Cunha M C P M, De Souza J P I, Nart F C. Reaction Pathways for

Reduction of Nitrate Ions on Platinum, Rhodium, and Platinum−Rhodium Alloy Electrodes [J]. Langmuir, 2000, 16(2): 771-7.
[12] Yang J, Sebastian P, Duca M, et al. pH dependence of the electroreduction of nitrate on Rh and Pt polycrystalline electrodes [J]. Chemical Communications, 2014, 50(17): 2148-51.
[13] Clark C A, Reddy C P, Xu H, et al. Mechanistic Insights into pH-Controlled Nitrite Reduction to Ammonia and Hydrazine over Rhodium [J]. ACS Catalysis, 2020, 10(1): 494-509.
[14] Liu H, Park J, Chen Y, et al. Electrocatalytic Nitrate Reduction on Oxide-Derived Silver with Tunable Selectivity to Nitrite and Ammonia [J]. ACS Catalysis, 2021, 11(14): 8431-42.
[15] Ohmori T, El-Deab M S, Osawa M. Electroreduction of nitrate ion to nitrite and ammonia on a gold electrode in acidic and basic sodium and cesium nitrate solutions [J]. Journal of Electroanalytical Chemistry, 1999, 470(1): 46-52.
[16] Flores E, Frías J E, Rubio L M, et al. Photosynthetic nitrate assimilation in cyanobacteria [J]. Photosynthesis Research, 2005, 83(2): 117-33.
[17] Liu H, Chen Z, Guan Y, et al. Role and application of iron in water treatment for nitrogen removal: A review [J]. Chemosphere, 2018, 204: 51-62.
[18] Liang J, Liu Q, Alshehri A A, et al. Recent advances in nanostructured heterogeneous catalysts for N-cycle electrocatalysis [J]. Nano Research Energy, 2022, 1: 9120010.
[19] Fan X, Xie L, Liang J, et al. In situ grown Fe_3O_4 particle on stainless steel: A highly efficient electrocatalyst for nitrate reduction to ammonia [J]. Nano Research, 2022, 15(4): 3050-5.
[20] He X, Li J, Li R, et al. Ambient Ammonia Synthesis via Nitrate Electroreduction in Neutral Media on Fe_3O_4 Nanoparticles-decorated TiO_2 Nanoribbon Array [J]. Inorganic Chemistry, 2023, 62(1): 25-9.
[21] Zhang S, Li M, Li J, et al. High-ammonia selective metal-organic framework-derived Co-doped Fe/Fe_2O_3 catalysts for electrochemical nitrate reduction [J]. Proceedings of the National Academy of Sciences of the United States of America, 2022, 119(6).
[22] Liu C, Zhang G, Zhang W, et al. Specifically adsorbed ferrous ions modulate interfacial affinity for high-rate ammonia electrosynthesis from nitrate in neutral media [J]. Proceedings of the National Academy of Sciences of the United States of America, 2023, 120(3): e2209979120.
[23] Lin H, Wei J, Guo Y, et al. Bi_1-$CuCo_2O_4$ Hollow Carbon Nanofibers Boosts NH3 Production from Electrocatalytic Nitrate Reduction [J]. Adv Funct Mater, 2024, 34(51): 2409696.

** Correspondence:*
Dr. Hua-Jun Shawn Fan
hfan@claflin.edu

Cheng Xiang Wang, JiaXin Liu1, Rui Zhu, Peng Yi Zhao, and Hua-Jun Shawn Fan, "AgO–CuO Composite Catalyst Enabling Efficient and Selective Nitrate-to-Ammonia Conversion," *International Research Journal of Advanced Engineering and Science*, Volume 11, Issue 2, pp. 152-162, 2026.